

RESEARCH

Open Access



Solute excretion improves trehalose uptake and desiccation tolerance of *Metarhizium brunneum* blastospores

Robin Dietsch^{1*}, Desiree Jakobs-Schönwandt^{1,2}, Luisa Blöbaum³, Marcus Persicke^{4,5}, Alexander Grünberger⁶ and Anant Patel¹

Abstract

In this study, a novel approach was developed to increase the intracellular trehalose concentration in *M. brunneum* blastospores by uptake from the medium, improving their desiccation tolerance. Briefly, placing the blastospores in a hypotonic environment induced solute excretion, allowing significantly increased trehalose uptake during subsequent trehalose treatment. Conductivity changes and GC–MS analysis revealed that glycerol and lactate excretion is triggered in a hypotonic NaCl solution. After hypotonic + trehalose treatment, intracellular glycerol, lactate, and glucose levels increased, while other desiccation-protective solutes remained unaffected. A fluorescence-based single-cell analysis of membrane stress and death during osmotic desiccation and rehydration showed that membrane stress and cell death were strongly amplified upon rehydration. Trehalose treatment reduced this amplification, while hypotonic + trehalose treatment minimised cell death and prevented a stress response during rehydration, though it increased membrane stress during desiccation. Newly formed germ tubes were identified as critical points of membrane failure during desiccation. Ultimately, the drying survival of blastospores was significantly improved by the hypotonic + trehalose treatment compared to untreated or trehalose-only-treated blastospores. In summary, this technique successfully enhanced blastospore desiccation tolerance and could be adapted to load cells with other solutes.

Keywords Desiccation tolerance, Drying, Formulation, Trehalose, Solute excretion, Microfluidic cultivation

*Correspondence:

Robin Dietsch

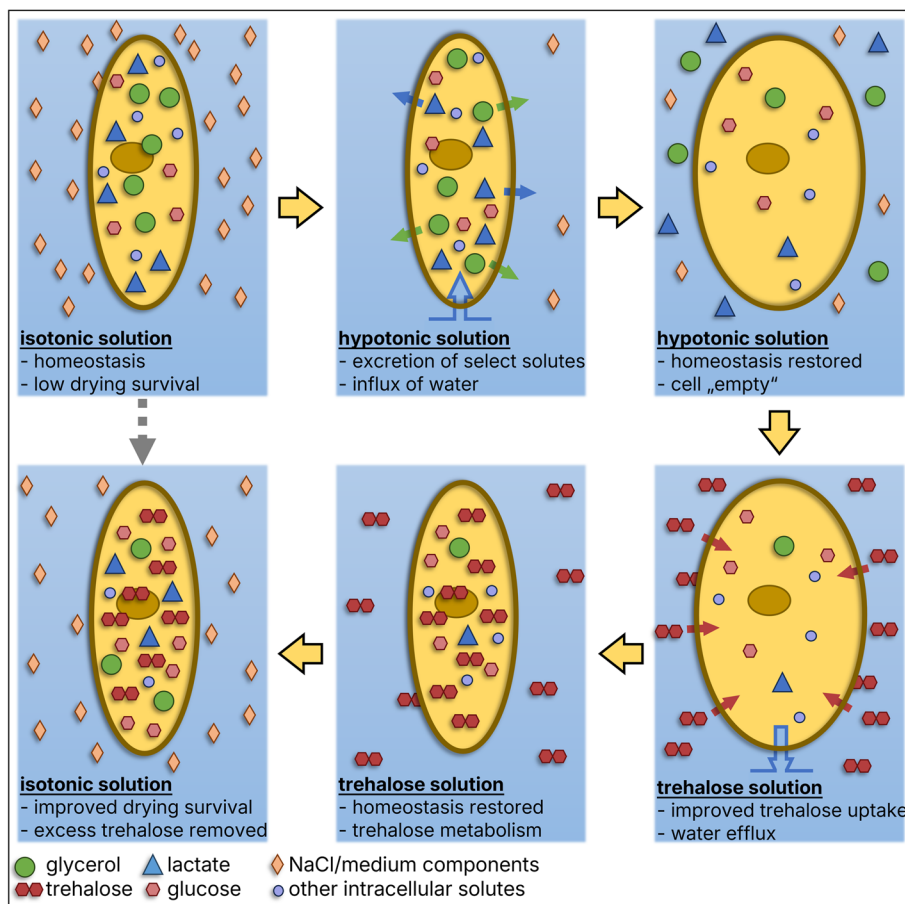
robin.dietsch@outlook.com

Full list of author information is available at the end of the article



© The Author(s) 2025. **Open Access** This article is licensed under a Creative Commons Attribution 4.0 International License, which permits use, sharing, adaptation, distribution and reproduction in any medium or format, as long as you give appropriate credit to the original author(s) and the source, provide a link to the Creative Commons licence, and indicate if changes were made. The images or other third party material in this article are included in the article's Creative Commons licence, unless indicated otherwise in a credit line to the material. If material is not included in the article's Creative Commons licence and your intended use is not permitted by statutory regulation or exceeds the permitted use, you will need to obtain permission directly from the copyright holder. To view a copy of this licence, visit <http://creativecommons.org/licenses/by/4.0/>.

Graphical Abstract



Introduction

Globally shifting climate conditions threaten safe and predictable crop production [1], necessitating increased pesticide use [2–4]. Simultaneously, an increasing number of fertilisers and pesticides are being outlawed yearly due to previously unknown risks to health and the environment [5]. As a result, the relevance of biological crop protection has steadily and globally increased [6]. Eco-friendly and sustainable approaches, such as biocontrol products, offer alternatives to the (over)use of conventional pesticides based on potentially harmful chemicals [7]. These include naturally occurring predators, microbial endophytes and entomopathogens, pheromones, extracts, or the like [7]. Biocontrol agents with live active ingredients especially suffer from limitations in storage stability. To compete commercially, a shelf life of approximately 1 year at room temperature should be guaranteed with minimal associated expenses [8–10]. For live fungal active ingredients, this requirement of commercial

viability leaves drying as the sole option for increasing product longevity.

Metarhizium brunneum blastospores, which can be applied for crop protection and enhance plant nutrient uptake, are an excellent example of a fungal biocontrol agent that significantly suffers from viability loss during drying and storage [11–13]. Like many endophytic entomopathogenic fungi (EPPFs), *M. brunneum* forms blastospores within an insect host. Their purpose is to rapidly multiply and starve the host of nutrients, leading to host death by mycosis [14]. A thin, flexible, nutrient-permeable cell wall [15, 16] and transmembrane sugar transporters [17–23] facilitate accelerated nutrient uptake. While these adaptations suit the parasitic lifecycle phase of many EPPFs, there is a trade-off in protection against abiotic stressors that are not typically encountered within the insect hemocoel. As a result, blastospores have severely reduced desiccation tolerance and are generally unsuited as live biocontrol agents. However,

their high growth rates in submerged fermentation, along with comparable or even greater infectivity than conidia or mycelium, make them industrially appealing [24–31].

In naturally desiccation-tolerant microorganisms, tolerance is achieved by several synergistic mechanisms [14, 32]. Compatible solutes, for example, protect proteins from aggregation by preferential exclusion [33–36], vitrification of the cytosol drastically decreases molecular motion [35–37], water replacement prevents membrane phase transition [38–40], and intrinsically disordered proteins have various other beneficial effects on cells during water stress [41–44]. The disaccharide trehalose, abundant in all known desiccation tolerant species, plays a central role in three of these mechanisms. It is a compatible solute [32, 45] and water replacer [38–40, 46] and induces vitrification in low water scenarios [36, 47]. Naturally, the efficacy of these modes of action in improving desiccation tolerance is concentration dependent [32, 36, 48–53].

Increasing the intracellular trehalose concentration in EEPF blastospores is typically achieved through hypertonic stress during fermentation [54, 55] and has become a standard practice in their production [26, 31, 56, 57]. A novel approach that relies on the natural ability of cells to regulate turgor pressure as a response to environmental hyper- or hypotonic shifts [32] and exploits the ability of blastospores to take up sugars quickly will be discussed in this study [17–23]. When cells are placed into a hypotonic solution, water will be imported, and select nonessential solutes are excreted to adapt to the new tonicity [58–60]. If these same cells were then placed into a hypertonic solution of trehalose, the disaccharide would be taken up by the cell alongside a water efflux from the cell, to regain osmotic homeostasis [17–23]. Hypothetically, cells should be able to accumulate trehalose at higher concentrations from the solution than without the preceding loss of other solutes via hypotonic treatment.

We hypothesise that by employing this technique, the intracellular trehalose level of *M. brunneum* blastospores can be significantly increased in general and compared to trehalose incubation without hypotonic pretreatment. Additionally, we expect this increase in intracellular trehalose to directly translate into an increased desiccation tolerance of *M. brunneum* blastospores. Furthermore, we investigate the amount and type of solutes excreted from the blastospores. In tandem with the hypotonic treatment, we will closely monitor dehydration processes of the treated cells with a powerful fluorescence-aided microscopic analysis, as employed in chip based microfluidic cultivation setups [61]. The small scale of microfluidics allows for high-replicate online monitoring, providing deeper insights into the treatment's effects on

the dehydration and rehydration process, as well as identifying critical time points or conditions where damage may occur.

The idea to 'empty' cells prior to 'loading' them with trehalose is a novel approach to impart desiccation tolerance and is described for the first time. It potentially enables higher intracellular trehalose mole fractions than naturally achievable by the organism via conventional preconditioning techniques. Furthermore, this approach should be applicable to all hypoosmotic stress-tolerant cell types with the ability to exchange solutes and is, therefore, potentially relevant to other microbiological and biotechnological fields as well.

Materials and methods

Aerial conidia production and harvest

Metarhizium brunneum CB15III was grown at 25 °C on potato dextrose agar (PDA, 39 g/L, Roth X931.2) plates until completely sporulated. The conidia were knocked or brushed loose with a sterilised brush and suspended by flushing the plates repeatedly with 0.1% Tween 80 (Carl Roth 9139.1). This conidial suspension was transferred from the plates into 1.5 mL reaction tubes (Starlab, TubeOne S1615-5500). These were stored at 4 °C for up to 2 weeks. All steps were carried out under sterile conditions.

Blastospore production

A preculture was obtained by inoculating a baffled 250 mL shaker flask filled with 75 mL fermentation medium (40 g/L AniPept™ Animox; 55 g/L D-glucose monohydrate, Roth 6887.3; 70 g/L polyethylene glycol 200, Roth 2631.2; pH=5.5, $a_w=0.987$) with 1 mL of aerial conidia suspension to a final concentration of 1×10^5 /mL and shaking at 150 rpm and 25 °C (IKA KS 4000 ic control) for 48 h. Shaker flasks, including biological replicates, were inoculated with 5% of the preculture and cultivated for 96 h under the same conditions and in the same medium as the preculture. This protocol was adapted from Krell, Jakobs-Schoenwandt [62]. Immediately after cultivation, the cultures were vacuum filtered through 12–15- μ m paper filters (VWR 516–0350) to remove all mycelium; 40 mL were collected in 50 mL centrifuge tubes (Greiner Bio-One, 227,270), cooled to, and kept at 4 °C. To remove the spent culture medium, the blastospore suspensions were centrifuged (5 min, 2150 \times g, 4 °C) and resuspended in pre-cooled 9 g/L sodium chloride solution (153 mM) (NaCl, Carl Roth P029.3) three times. Keeping the cells at 4 °C was crucial to prevent unwanted solute excretion. All steps were carried out under sterile conditions.

Hypotonic and trehalose incubations

For the hypotonic and trehalose incubations, blastospore suspensions were centrifuged as described above and resuspended in a solution of either 0.72 g/L NaCl (12.32 mM, pH ca. 5.5 (not adjusted)) or 100 g/L trehalose dihydrate (260 mM) (GOURMET VERSAND, 13,779, pH 5.5 (adjusted with 100 mM NaOH or HCl)) in ultrapure water. Then, they were slowly shaken for 20 min at 20 °C to avoid sedimentation. The blastospores were washed thrice before transfer from the hypotonic to the trehalose solution. All steps were carried out under sterile conditions. Table 1 displays the different treatment procedures referred to in the manuscript. Hypotonic treatment is sometimes referred to on its own but is usually conducted as part of the hypotonic + trehalose treatment except in the solute efflux conductivity analysis.

Dehydration and rehydration

Dehydration took place in detached and sterilised lids of 1.5 mL reaction tubes (Starlab, TubeOne S1615-5500) filled with 100 µL of blastospores suspended in 9 g/L NaCl or 100 g/L trehalose. The lids were then simultaneously air dried in a 45 L container with an air flow of 10 L/min and 5% relative humidity (rh). All samples were dried at 20 °C to a water activity of 0.30–0.35 (LabMaster-aw, Novasina) or for a maximum of 48 h. The drying apparatus was constructed of a transparent, lidded container (Samla 45 L, Ikea), installed with an inlet hose nozzle and an outlet hole of 3 mm diameter. The lid was sealed against the container with silicone paste and secured with weights. The air was provided via an in-house air compression system that dehumidified the air to 5% rh and was connected to the container inlet nozzle via air tubing and a gas flowmeter (1–10 L/min, Joyzan). The air was sterile filtrated (Midisart™ 2000 PTFE Air Filter, Sartorius) before the inlet nozzle.

To rehydrate dried blastospores, the lidless reaction tubes were filled with 1 mL of 9 g/L NaCl at 20 °C, and the lids with the dried blastospores were carefully placed upon them. The tubes were then immediately inverted and vortexed in this position for 1 min or until all dry residue from the lid was dissolved or suspended. All steps

during de- and rehydration were performed under sterile conditions and at 20 °C.

Cell counting

Blastospores were counted in a ‘Neubauer Improved’ cell counting chamber (Marienfeld Superior) at $\times 40$ magnification using a transmitted-light microscope (Axiostar Plus, Zeiss).

Viability/CFU analysis

The blastospore viability was determined via CFU analysis. Blastospore suspensions were diluted in 9 g/L NaCl solutions to a total amount of approximately 200 viable blastospores per PDA plate. Sensible dilution factors were determined by cell counting and estimation of survival rates based on pre-experiments (data not shown). Prior to drying, reference samples were taken from all replicates and plated at 200 blastospores per plate to determine the viability of the drying process. The plates were sealed with PARAFILM® and kept at 25 °C for 96 h, until all colonies were visible and easily countable. The plates were checked again after another 24 h if any colonies were missed. The colonies on all plates were counted and survival was determined for all samples utilising the reference samples. All samples were plated and counted in duplicate in addition to the experimental replicates. All steps were carried out under sterile conditions. In case of dried and rehydrated blastospores, the CFU analysis immediately followed rehydration.

Solute efflux conductivity analysis

For the solute conductivity analysis, lyophilised blastospores were suspended in 30 mL of 154 mM NaCl at either 1×10^7 , 5×10^7 , or 1×10^8 viable blastospores/mL at 20 °C in 50 mL centrifuge tubes. The conductivity (σ_{mi}) of the suspension was measured (Thermo Orion™ STAR A3295), and two 10 µL samples were taken for viability determination (*viab.*). Then, the blastospores were pelleted by centrifugation (5 min, 2150 \times g, 4 °C), 27.6 mL of the supernatant were removed, replaced with ultrapure water (Elix Advantage 5, Merck), and the blastospores were resuspended, resulting in a 0.72 g/L NaCl (12.32 mM) solution/suspension. After slow shaking for 20 min at 20 °C, the conductivity was measured again (σ_{hyp}) and two 10 µL samples were taken for viability determination (*viab.*). The blastospores were then autoclaved and rigorously vortexed for 2 h with 10 mL of 0.5 mm glass beads, and another conductivity measurement was taken (σ_{dead}). The cell disruption was confirmed microscopically. The procedure was performed in quintuplicate for every concentration and a cell free control (σ_{ctrl}) and repeated twice with similar results (Supplementary Materials 1).

Table 1 The different treatment procedures applied to *M. brunneum* blastospores, referred to throughout the study. All treatments were administered for 20 min

	Trehalose (tre. treat)	Hypotonic (hyp. treat.)	Hypotonic + trehalose (hyp. + tre. treat.)
1.	100 g/L trehalose $a_w=0.988$	0.72 g/L NaCl $a_w=0.997$	12.32 mM NaCl $a_w=0.997$
2.	-	-	100 g/L trehalose $a_w=0.988$

The delta conductivities shown in Fig. 1 were calculated using the following formulae.

$$d\sigma_{\text{hyp}} = \frac{(((\sigma_{\text{hyp}} - \sigma_{\text{ini}}) - (\text{mean}(\sigma_{\text{hyp,ctrl}} - \sigma_{\text{ini,ctrl}}))) - (\sigma_{\text{dead}} * 1 - \text{viab.}))}{\text{viab.}} \quad (1)$$

$$d\sigma_{\text{dead}} = (\sigma_{\text{dead}} - \sigma_{\text{ini}}) - (\text{mean}(\sigma_{\text{dead,ctrl}} - \sigma_{\text{ini,ctrl}})) \quad (2)$$

Finally, the percentage of released solutes was determined as follows: $\%rs = \frac{d\sigma_{\text{hyp}}}{d\sigma_{\text{dead}}} * 100$.

GC–MS analysis of solutes

For GC–MS solute analysis, blastospores in quadruplicate biological replicates were harvested and either trehalose or hypotonic + trehalose treatment was conducted in 50 mL centrifuge tubes filled to 30 mL immediately after harvest. The blastospores were neither resuspended in NaCl nor cooled to 4 °C. Samples were taken immediately after harvest (untreated control), after trehalose treatment (tre. treat.), and during hypotonic + trehalose treatment after the hypotonic incubation (hyp. treat.) and after the trehalose incubation (hyp.+ tre. treat.).

For sampling, 2 mL of blastospore suspension was transferred to 2 mL reaction tubes and washed with 70 g/L ice cold PEG200 (1.5 min, 2150×g, 4 °C). The suspended blastospores were pelletised, the supernatant thoroughly decanted, and the pellet immediately frozen in liquid nitrogen. The pellets were then lyophilized (Christ, Osterode am Harz, Germany), and the dry weight was determined for normalisation. Subsequently, the metabolites were extracted and derivatised. For this purpose, the blastospore pellet was first mixed with 10 µM ribitol in 1 mL 80% MeOH and then ribolysed (Precellys 24, Bertin Technologies SAS, Montigny-le-Bretonneux, France). After subsequent centrifugation, the supernatant was dried in a nitrogen stream and derivatised using the Gerstel robot (MPS Robotic, Mülheim an der Ruhr, Germany) in a 2-step procedure. This included first the addition of 75 µL of a 30 mg/mL methoxyamine in pyridine solution followed by a 90 min reaction at 37 °C and an addition of 75 µL MSTFA (Macherey–Nagel, Düren, Germany) with a 30 min incubation time at 37 °C.

The derivatised samples were analysed by gas chromatography-mass spectrometry (GC–MS; Trace 1310 GC coupled to a TSQ9000 mass spectrometer, Thermo Fisher Scientific, Dreieich, Germany) in electron impact positive ionisation mode at 70 eV. For separation, an OPTIMA 5 ms column (30 m×0.25 mm i.d. 0.25 µm,

Macherey–Nagel, Düren, Germany) with a helium flow of 1 mL/min was used. A sample volume of 1 µL was

injected at 250 °C in splitless mode at a transfer line temperature of 250 °C. The temperature programme was set to 80 °C for 3 min, followed by a ramp of 5 °C/min to 325 °C. Masses from 50 to 750 m/z were measured in full scan mode. Additionally, blank samples without biological material and reference metabolites were measured, and retention indices [63] determined. The solutes were identified by comparison of their retention indices, mass spectra, and characteristic qualifier and quantifier masses to references (most of them listed in Plassmeier, Barsch [64]), the Golm metabolome database [65, 66], as well as mass spectral and retention time index libraries [67]. Any reference substances were purchased from Sigma-Aldrich, Merck, Roth (Karlsruhe, Germany) or Macherey–Nagel (Düren, Germany). Peaks not occurring in the blanks and with a signal-to-noise ratio of at least 3 were quantified in terms of peak areas in relation to the internal standard ribitol and the pellet dry weight with the software Xcalibur (Version 4.2, Thermo Fisher Scientific, Dreieich, Germany) considering only peaks occurring in at least 50% of the replicates of one treatment. Peak areas were transformed by log (peak area + 1).

The fold change of the normalised solute peak areas of all treatments were calculated in relation to the control peak areas. To facilitate visualisation in Fig. 2, a base 10 logarithmic scale was chosen, equally displaying the ranges from 0.1 to 1 and 1 to 10, wherein all fold changes were encompassed.

Lastly, trehalose standards were measured separately but with the same column and method to approximate the amount of intracellular trehalose. The standards contained 0.2 ng, 2 ng, 20 ng, 200 ng, 2000 ng, and 20,000 ng of trehalose.

Microfluidic analysis

Microfluidic chip fabrication, flow profile establishment, and all other preparations were done in accordance with Blöbaum, Täuber [68]. In short, a polydimethylsiloxane (PDMS)-chip was fabricated, containing the microfluidic structures. The structures are a modification of previously published dynamic microfluidic single-cell cultivation designs, enabling the switching between

four different media conditions [69]. Another modification was the spatial separation between the control and switching cultivation structures, which now contain 6 arrays of 23 growth chambers each. The experimental treatments were conducted in the centre structure, while the outside structures were used as dedicated positive and negative controls. The growth chamber dimensions were $90 \times 0.7 \times 80 \mu\text{m}$ (width \times height \times length), and the channel height was $11 \mu\text{m}$.

$$ctcf = \text{integrated density} - (\text{area of selected cell} * \text{mean background fluorescence})$$

The chip was placed into the temperature-controlled incubation cage (OKO-H201, OKO Lab) of an automated inverted microscope (Nikon Eclipse Ti2, Nikon). The chip was loaded with $1 \times 10^7/\text{mL}$ blastospores, all in- and outlets were connected to the media reservoirs or waste collection, the temperature was set to $25 \text{ }^\circ\text{C}$, and suitably loaded chambers for live cell imaging during the experiment were identified. Twelve chambers were chosen for the treatment and 6 for every control. All chosen chambers contained at least 6 and up to 43 blastospores. The final sample size (total number of cells) is given in the description of Fig. 3.

Phase-contrast and fluorescent images were taken every 10 min using a $100\times$ oil objective (CFI P-Apo DM Lambda, Nikon) and two filters: GFP (Ex 472/30; DM 495; Em 520/35, Nikon) and mCherry (Ex 562/40; DM 593; Em 640/74, Nikon). Phase-contrast images were captured for 80 ms at 10% intensity using the microscope's DIA illumination, GFP images were captured for 20 ms at 15% intensity, and mCherry images for 20 ms at 10% intensity using a LED-based light source for episcopic fluorescence (Sola SE II Set, Lumencor). All experimental solutions contained $1 \mu\text{g}/\text{mL}$ propidium iodide (PI) and $1.5 \mu\text{g}/\text{mL}$ bis-(1,3-dibutylbarbituric acid) trimethine oxonol (BOX), adapted from Simonin, Beney [70] and Krämer, Wiechert [71] and were sterile filtrated before use. Changing the pressure on the pressure-driven pumps (Line-up EZ series, Fluigent) enabled dynamic solution changes in the chip's centre cultivation structure. The image acquisition was terminated after 40 h for hypotonic + trehalose treatment and after 70 h for trehalose treatment and untreated blastospores; however, only the approximately first 15 h are reliable for measurements due to excess mycelium growth and channel plugging. Every treatment was conducted on a separate chip. Table 2 details the treatment procedures.

The analysis of the .nd2 image files created by the microscope software (NIS Elements AR) was performed with Fiji [72]. The file of each treatment was split into three-channelled hyperstacks of single growth chambers

at select timepoints. All growth chamber images were stabilised and all blastospores within a chamber were manually and individually selected as regions of interest as well as three continuously cell-free background areas in every chamber. Finally, with the integrated density, area of the selected cell, and the mean grey value of the background, all given by Fiji's 'measure' command, the corrected total cell fluorescence (ctcf) was calculated for every blastospore [73].

Drying survival analysis

To determine the influence of the treatments on blastospore drying survival, trehalose-treated, hypotonic + trehalose-treated, and untreated (control) blastospores were dried and rehydrated in quintuplicate, and the viability of every replicate was determined via colony forming units (CFU) analysis. The experiment was repeated twice with the same results.

Statistical analyses

All statistical analyses were conducted in R [74–78]. For the solute efflux analysis, linear regressions were performed on the delta conductivity. An interaction term for 'death/destruction' was included to identify a significant difference between 'hyp.treat.' and 'death/destruction'. The values for p , F , n , and R^2 for the regressions as well as the p -value of the interaction term are included in figure descriptions. The datasets of the GC–MS analysis were analysed via ANOVA. A Shapiro–Wilk test was performed to test for normal distribution of the residuals and a Levene test was performed to test for homogeneity of variances. If normal distribution of the residuals was not given, a Kruskal–Wallis test with a posthoc Dunn's test was performed instead. If the variances were inhomogeneous, a Welsh ANOVA with a pairwise t -test was performed instead. If the residuals were normally distributed and the variances were homogenous, the ANOVA results were analysed with a posthoc Tukey test. A generalised linear model (family = quasibinomial) was used to identify significant differences in the proportional viability data of the drying survival analysis. Significant differences in figures are indicated by lowercase letters or in the figure descriptions. Values for p and n are denoted in the respective figure descriptions.

Results

The treatment described in this study relies on three separate conditions that, to successfully improve desiccation tolerance, must be satisfied in succession. (i) The blastospores must excrete significant amounts of solutes in the

hypotonic environment. (ii) Trehalose must be taken up in significant quantities. (iii) The absorbed trehalose must protect the blastospores during drying and rehydration. Not only must these conditions be satisfied, but they should also ideally result in greater viabilities compared to a simple trehalose incubation. The conducted experiments were chosen to test these hypotheses step by step.

Solute efflux conductivity analysis

To discover the extent to which blastospores shed solutes in the hypotonic environment, the change in conductivity of a low salt medium was monitored, after blastospore transfer and subsequent destruction. These conductivity changes are shown in Fig. 1.

Figure 1 details the conductivity changes of blastospore dispersions after the initial hypotonic treatment (partial solute excretion) and then after cell destruction (complete solute release) for three different blastospore concentrations. The conductivity increased with blastospore concentration following both hypotonic treatment and cell destruction. However, while the blastospore concentration quintupled ($1 \times 10^7/\text{mL} \rightarrow 5 \times 10^7/\text{mL}$), the delta conductivity increased 3.6-fold for shocked and 3.5-fold for killed/destroyed blastospores. Likewise, a doubling in concentration ($5 \times 10^7/\text{mL} \rightarrow 1 \times 10^8/\text{mL}$) only led to a 1.6-fold and 1.7-fold increase in delta conductivity for shocked and killed/destroyed blastospores,

respectively—approximately 70% to 85% of the expected increases.

Cell destruction after hypotonic treatment uniformly increased the delta conductivity by approximately 21–24% for every sample, independent of blastospore concentration, implying a release of approximately 76–79% of all charged internal solutes during hypotonic treatment.

GC–MS analysis of solutes

GC–MS analysis was conducted for a broad spectrum of solutes to gain insight into the nature of released solutes. Figure 2 shows the fold changes in the intracellular concentrations of trehalose, glycerol, lactate, mannitol, and glucose after hypotonic treatment, trehalose treatment, and hypotonic+trehalose treatment compared to the untreated control. The fold changes of maltose and ribose-5-phosphate are shown in the Supplementary Materials 2.

Figure 2 shows the fold changes of blastospores' intracellular concentration of trehalose and other intracellular metabolites after treatment, hypotonic treatment, and hypotonic+trehalose treatment. The hypotonically treated blastospores were sampled from the same set of blastospores that was trehalose treated afterwards as part of the hypotonic+trehalose treatment.

In general, hypotonic treatment caused a significant decrease in glycerol and lactate concentration and no significant increases. Trehalose-treated blastospores contained

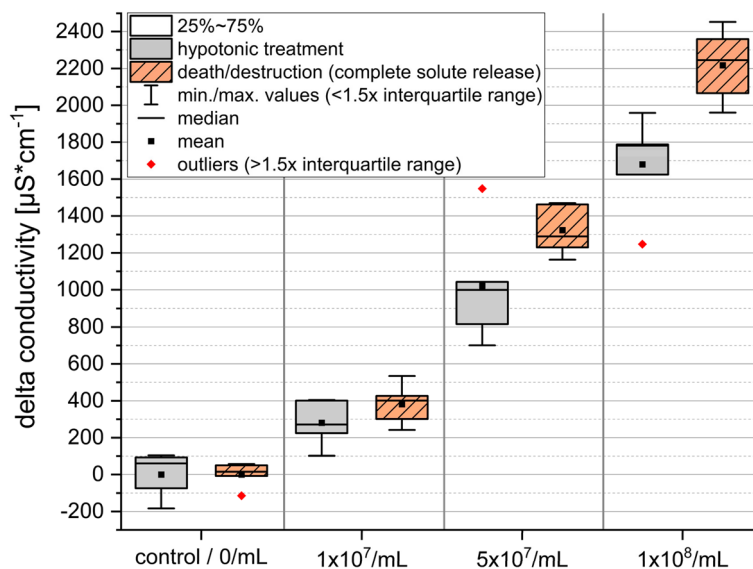


Fig. 1 The conductivity increase (delta conductivity) that occurred due to blastospore solute release after media dilution from 154 mM NaCl to 12.32 mM NaCl (hypotonic shock) and after blastospore death and integrity disruption by heat and mechanical stress (death/destruction). The blastospore concentrations are shown on the unscaled x axis. No blastospores were present in the control. The data was normalised to the control and the survival rates after hypotonic shock were accounted for in the calculations. $n=5$. According to linear regression, the blastospore concentration had a significant influence on the delta conductivity of hypotonic shock (adj. $R^2=0.8928$ $F_{1,18}=159.2$; $p=2.239^{-10}$) and death/destruction (adj. $R^2=0.9659$ $F_{1,18}=538.4$; $p=7.306^{-15}$). The effect of concentration was modified by death/destruction of the cells ($p=0.00269$). All outliers were included in the linear regression and interaction term

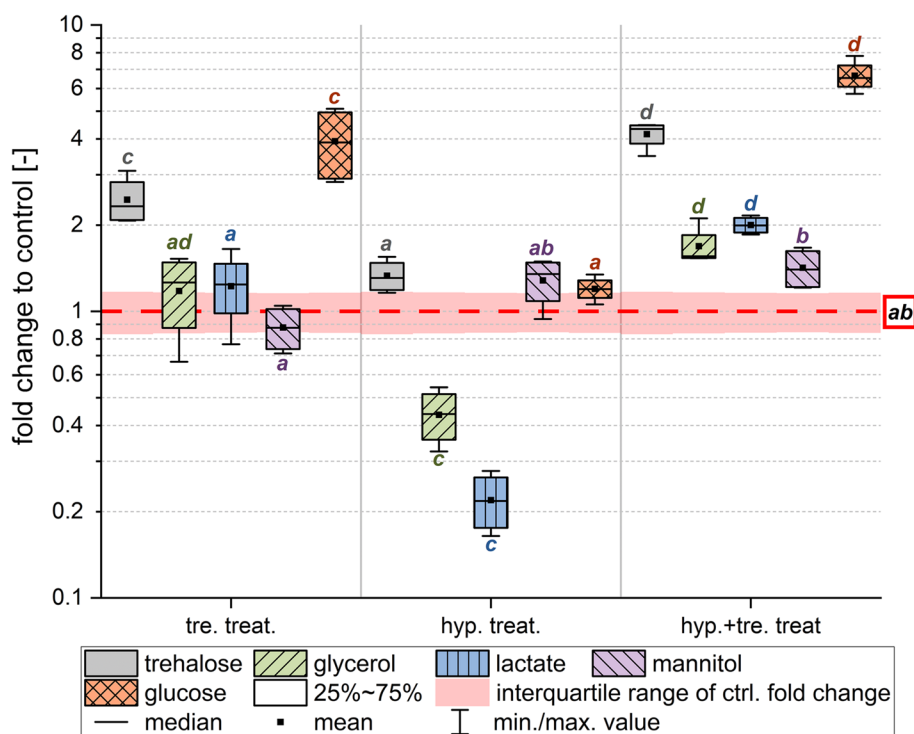


Fig. 2 Depicted is the fold change of GC-MS normalised peak areas of intracellular solutes to the untreated control (red dashed line) after, trehalose treatment, hypotonic treatment, or hypotonic + trehalose treatment. The red transparent area along the control line indicates the interquartile range concentrations of the untreated control. Lowercase letters indicate significant differences between the same solutes after the different treatments and to the control, but not to other solutes ($n=4$, $p < 0.05$). Exact p -values, F -values, and employed tests for every solute are given in the Supplementary Materials 2

significantly more trehalose and glucose than the control. Compared to hypotonic treatment, trehalose treatment significantly increased trehalose, glycerol, lactate, and glucose concentrations. After the completed hypotonic + trehalose treatment, trehalose, glycerol, lactate, and glucose concentrations were significantly increased compared to the control and compared to trehalose treatment. After hyp. + tre. treatment, blastospores contained approximately 9.98 $\mu\text{g}/\text{mg}$ trehalose per blastospore dry weight.

Overall, trehalose treatment only affected trehalose and its metabolite glucose. The hypotonic incubation, as expected, induced significant decreases of select solutes, in this case lactate and glycerol. Most solutes, however, were unaffected. Only when the hypotonic incubation was followed by a trehalose incubation in hyp. + tre. treatment, trehalose, glucose glycerol, and lactate concentrations increased significantly.

Emulated drying process on single-cell level

With its unique ability to preserve cell membrane fluidity in a dehydrated state, trehalose can protect cells from the strong physical forces acting on their, then typically rigid, cell membrane during rehydration [38–40, 46]. Microfluidic single-cell cultivation was chosen to confirm this mode

of action's compatibility with *M. brunneum* blastospores, to quantify this effect, and to gain a more detailed understanding of the impact of the hypotonic + trehalose treatment on blastospores in general. The emulation of a drying process by osmotic de- and rehydration in the microfluidic environment enabled fluorescence-based membrane stress and death marking during all steps of the de- and rehydration procedure. The fluorescence signal progression of the stress and death markers is depicted in Fig. 3a.

Figure 3a shows the mean corrected total cell fluorescence of stained blastospores, dependent on the treatment and the progress of the desiccation process. PI fluorescence (red) indicates cell death, while BOX fluorescence (green) indicates membrane stress/depolarisation. There was a 20 min offset between the untreated blastospores (dotted lines), tre. treat. (dashed lines), and hyp. + tre. treat. (solid lines) graphs, with the hyp. + tre. treat. graph beginning at $t=0$ min, the tre. treat. graph beginning at $t=20$ min, and the control graph beginning at $t=40$ min. This accounted for the control and tre. treat not being subjected to the hypotonic incubation and the control also not being subjected to the trehalose incubation. For all treatments, dehydration uniformly began at 2 h and 40 min. All treatment procedures are outlined in Table 2.

Most striking is the universally sharp increase in PI-ctcf immediately following rehydration. The untreated PI-ctcf increase upon rehydration was 12.8 times greater than after trehalose treatment and 45.9 times greater than after hypotonic + trehalose treatment. This PI-ctcf progression was only somewhat mirrored by the BOX-ctcf. While the untreated and tre. treat. BOX-ctcf also increased sharply upon rehydration, the hyp. + tre. treat. BOX-ctcf even decreased. Overall, the resulting untreated BOX-ctcf was 5.5 times greater than after trehalose treatment and 27.4 times greater than after hypotonic + trehalose treatment. The osmoprotective properties of trehalose could already be seen during the desiccative phase, in which the untreated blastospores' mean PI-ctcf steadily increased, while that of treated blastospores did not. Membrane stress universally increased during the desiccation. Interestingly, hyp. + tre.-treated blastospores suffered higher membrane stress than trehalose-treated blastospores. Both treatments, however, prevented much desiccative stress, when compared to untreated blastospores with the untreated BOX-ctcf being 5.2 times and 2.5 times higher than that of tre. treat. and hyp. + tre. treat, respectively. Lastly, the hypotonic + trehalose treatment initially negatively affected the blastospores, as stress levels spiked during both incubations. This evidently stressful hypo-to-hypertonicity switch could have also caused the elevated BOX-ctcf during desiccation.

Interestingly, trehalose-treated blastospores only contained 1.7 times less trehalose (Fig. 2) than hypotonic + trehalose-treated blastospores but displayed 5.0 and 3.6 times higher BOX- and PI-ctcfs. Untreated blastospores contained 4.2 times less trehalose than hypotonic + trehalose-treated blastospores (Fig. 2) and displayed 27.4 and 45.9 times higher BOX- and PI-ctcfs upon rehydration.

In addition to the quantification of trehalose's protective effects, the microfluidic cultivation enabled close visual observation of the entire process. Figure 3b consists of images of two microfluidic chambers at the end of the desiccation phase ($t=4.5$ h). Untreated blastospores are shown on the left and hypotonic + trehalose-treated blastospores on the right. Some blastospores from both treatments formed germ tubes either during or before the experiment and predominantly those blastospores were fluorescent. While the germinated blastospores from the control almost all fluoresce with BOX and/or PI, the

hypotonic + trehalose-treated, germinated blastospores mainly fluoresce with BOX at the germ tubes. There are two examples in the control (yellow ovals) where blastospores were not uniformly fluorescent. The germ tubes showed a PI signal while the rest of the blastospores were BOX-stained or remained unstained. Two hypotonic + trehalose-treated blastospores appear to be in the very early stages of germ tube formation, where a germ tube is not yet or barely visible (red oval). This phenomenon occurred in several of the observed chambers. Other instances are depicted in the Supplementary Materials 3. In addition to being another example of the protective effects of trehalose, this is also the first report of a previously undiscovered vulnerability during dehydration in the form of newly formed germ tubes.

Increased desiccation tolerance

After showing that all conditions for the hypotonic + trehalose treatment to increase desiccation tolerance were met, treated blastospores were tested for viability in a real drying process. The treatments included an untreated control, trehalose-treated blastospores with and without the trehalose solution removed before drying, and hypotonicity pre- and trehalose-treated blastospores with and without the trehalose solution removed prior to drying. The results are presented in Fig. 4.

Figure 4 shows a significant increase in post drying viability with all treatments. Simple trehalose incubation with removal of the trehalose solution increased the viability to 21.5%. Hypotonic + trehalose treatment and removal of the residual trehalose increased the viability to 40.5%. Not removing the trehalose prior to drying further increased the viability to 51.5% without and 71.5% with prior hypotonic treatment. The control group's viability was 6.4%.

In addition to the viability, the final water activity (a_w) of the samples was measured after drying to the target water activity of <0.35 or after a maximum of 48 h. The results are shown in Table 3.

Besides the significant increase in viability, another treatment-dependent effect could be observed. Table 3 reveals that not all samples reached the targeted water activity of <0.35 within 48 h. The samples that failed to do so were those dried in residual trehalose with water

(See figure on next page.)

Fig. 3 a The mean corrected total cell fluorescences of bis-(1,3-dibutylbarbituric acid) trimethine oxonol (BOX) and propidium iodide (PI) over the course of the microfluidic desiccation process of untreated, trehalose-treated, and hypotonic + trehalose-treated blastospores. The graph is expanded to display the first 6 h of the experiment in which the hypotonic treatment (grey background area), the trehalose incubation (green background area), and the high-salt desiccation (orange background area) occur. The preceding cultivation in and subsequent rehydration to growth medium is indicated by the blue background. The full graph is shown in a miniature view to show the development beyond 6 h. All ctcfs were normalised to zero at t_0 . **b** Untreated and hypotonic + trehalose-treated blastospores at the end of the desiccation ($t=4.5$ h). The images are compositions of the phase contrast, green, and red fluorescence channel images. The yellow and red ovals enclose points of interest, specified in the text

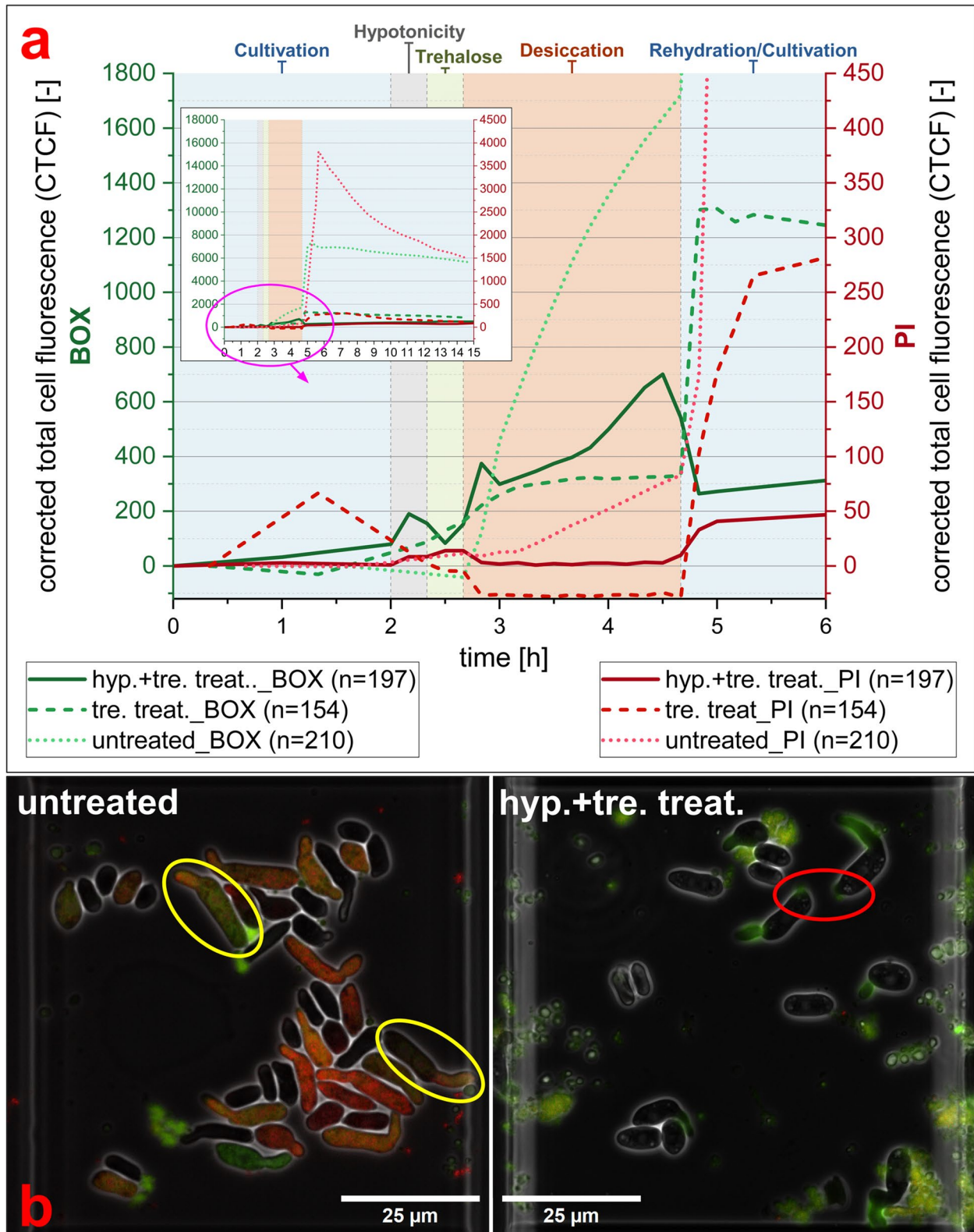


Fig. 3 (See legend on previous page.)

Table 2 Overview of the treatment procedures applied to *M. brunneum* blastospores in the microfluidic chip system

Media changes	Ctrl-	Ctrl+	Untreated	Trehalose treatment	Hypotonic + trehalose treatment
0	7 M MgCl ₂ (∞)	Medium (∞)	Medium (2 h)	Medium (2 h)	Medium(2 h)
1	-	-	7 M MgCl ₂ (2 h)	100 g/L trehalose(20 min)	12,32 mM NaCl (20 min)
2	-	-	Medium (∞)	7 M MgCl ₂ (2 h)	100 g/L trehalose (20 min)
3	-	-	-	Medium (∞)	7 M MgCl ₂ (2 h)
4	-	-	-	-	Medium (∞)

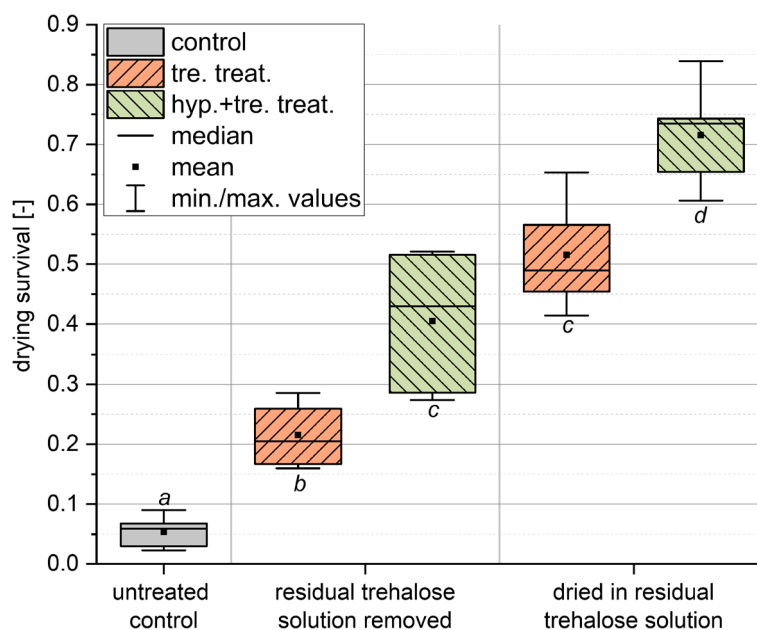


Fig. 4 Drying survival of untreated (control), trehalose-treated (tre. treat., and hypotonic + trehalose-treated (hyp. + tre. treat) blastospores of *M. brunneum*, with the residual trehalose solution from the treatments either removed and exchanged for 0.9% NaCl or not. Lowercase letters indicate statistically significant differences according to a general linear model ($n=5, p < 0.05$). Estimated differences of the logit model, standard errors and exact p -values against all treatments are given in the Supplementary Materials 4. The data was normalised to the viability of the respective treatment before drying

Table 3 The final water activities (a_w) of the samples post drying and the drying duration

Treatment	a_w of dried samples	Drying duration
Untreated control, dried in 0.9% NaCl	0.306	16 h
tre. treat., dried in 0.9% NaCl	0.311	16 h
tre. treat., dried in 10% trehalose	0.460	48 h
hyp. + tre. treat., dried in 0.9% NaCl	0.349	17 h
hyp. + tre. treat., dried in 10% trehalose	0.429	48 h

activities of 0.460 and 0.429, respectively. After 18 h of drying, the water activities of the control and trehalose treatment reached 0.306 and 0.311, respectively. After 19 h of drying, the water activity of trehalose + hypotonic treatment reached 0.349.

Discussion

The presented treatment relies on three conditions that must be satisfied in order to achieve the desired outcome: solutes must be excreted, trehalose must be taken up, and trehalose must be able to increase desiccation tolerance in *M. brunneum* blastospores.

The first condition was satisfied by triggering blastospore solute excretion via hypotonicity. The results shown in Fig. 1 clearly indicate a release of internal solutes from the blastospores in all three blastospore concentrations. It is known that cells possess the ability to excrete nonessential solutes in a hypotonic environment to reinstate tonic homeostasis [58–60]. Likely, a charged solute is selectively excreted. That this solute, however, causes a conductivity increase approximately four times greater than all remaining internal solutes, including all ions, is questionable.

Likely, many of a blastospores internal solutes, organelles, and intracellular building blocks suppress electrical conductivity, just as glycerol does and their combined release upon cell destruction dampens the expected conductivity increase upon cell destruction [79]. Unfortunately, there are no reports in literature regarding the percentage of solute expulsion. Conductivity changes via premature cell death in the 'hypotonic shock' phase of the experiment were accounted for and can therefore be ruled out as an influencing factor. The non-proportional relationship between the delta conductivities and the blastospore concentration could be explained by a non-linear conductivity curve of the excreted solute mixture or caused by pH changes, resulting in the protonation of the charged solute for example [80].

The GC–MS analysis then gave insight into the identity of the released solutes and revealed that of the analysed solutes, only three significantly decreased in intracellular concentration after hypotonic treatment. These were glycerol, lactate, and ribose-5-phosphate (Fig. 2 and Supplementary Materials 2). Whether this decrease in intracellular concentration is caused by metabolic conversion or a release is unclear. As glycerol is released by many yeasts and other fungi as a response to hypotonic stress [58–60], the observed decrease is likely the result of cellular excretion but cannot cause the increase in conductivity in Fig. 1 [81, 82]. More likely, lactate, which also decreased in significant amounts, is the cause. It increases electrical conductivity in solutions [83] and, as an end product of energy metabolism, is likely expendable to the blastospores in hypotonic stress situations. Furthermore, there already is evidence of some entomopathogenic fungi being able to secrete lactic acid [84], pointing towards a lactate release over lactate metabolism. Lastly, there was significant decrease of ribose-5-phosphate (Supplementary Materials 2), accompanied by an insignificant decrease in ribulose-5-phosphate (data not shown). Because of its importance in the pentose phosphate pathway and the parallel decrease of ribulose-5-phosphate, the concentration drop is likely caused by metabolic shifts.

The second condition was satisfied by blastospore incubation in a highly concentrated trehalose solution. Here the GC–MS enabled trehalose uptake evaluation and, additionally, observation of the treatment's effects on other key solutes involved in fungal desiccation tolerance [51, 59, 85–89]. GC–MS analysis revealed a significant increase in trehalose concentration after trehalose treatment and hypotonic + trehalose treatment. In both cases, this increase was expected, as blastospores likely incorporate trehalose as an energy source or to adapt to the osmolarity of the high trehalose concentration. Interestingly, hypotonic + trehalose treatment yielded a significantly higher trehalose increase

than just trehalose treatment, lending credibility to the hypothesis of increased intracellular capacity after hypotonic incubation. Considering all findings discussed so far, hypotonic + trehalose treatment appears to exchange intracellular lactate for trehalose. While trehalose is a compatible solute, water replacer, and glass former, lactic acid is not. Therefore, this simple exchange is already a net benefit for the blastospores regarding desiccation tolerance. Furthermore, according to the water replacement hypothesis, trehalose is unique among compatible solutes in its ability to prevent cell membrane phase transition near absolute dehydration [90–92], as encountered in drying processes for long term product storage. Typically, however, entomopathogenic fungi rely on a mixture of sugars and polyols to protect themselves against desiccative stress [13, 55, 85, 89, 93]. Potentially sacrificing protectant variety to increase trehalose concentration could prove detrimental overall. Figure 2, however, shows that, mannitol, glucose, glycerol, and maltose (Supplementary Materials 2), all associated with fungal desiccation tolerance [14], do not significantly decrease in concentration, or even increase in concentration after hypotonic + trehalose treatment. The strong increase in glucose, mirroring the trehalose increase, hints at the partial metabolism of trehalose during the hypertonic trehalose incubation, possibly to rebuild intracellular glycerol, which also significantly increased in concentration only after hypotonic + trehalose treatment. Perhaps, the reverse and larger difference in tonicity through the hypotonic + trehalose treatment amplified the blastospores' stress response, increasing the amount of protective molecules synthesised. This in turn would, as a secondary effect, further increase desiccation tolerance, as glycerol has been shown to amplify trehalose's protective effects [47, 94]. Fine tuning the difference in tonicity and finding optimal solute compositions to offer after hypotonic incubation could be key to further increasing desiccation tolerance.

After hypotonic + trehalose treatment and the resulting increase in intracellular trehalose, the blastospores contained approximately 10 µg/mg trehalose per blastospore dry weight, or 1%. *Saccharomyces cerevisiae*, conditioned for dry storage, ideally contains approximately 15% [95, 96], suggesting ample room for improvements in intracellular trehalose concentration. However, in their studies on increasing the intracellular trehalose content of *Metarhizium anisopliae* by optimising fermentation conditions and osmotic preconditioning, Hallsworth and Magan [97], Hallsworth and Magan [98], and Hallsworth and Magan [99] reported only one instance of trehalose concentrations reaching approximately 15 µg/mg in conidia grown on trehalose in excess. In all other instances, the concentrations did not exceed 8 µg/mg [97–99]. Krell et al. report a concentration of 0.5 µg/mg in *M. brunneum* [89]. This suggests that the capacity for

trehalose uptake in *Metarhizium* spp. in the magnitude of 15% like *S. cerevisiae* is not feasible.

The last condition was shown to be satisfied in the microfluidic desiccation process, utilising a fluorescent membrane stress and death marker. If not properly protected, cell membranes undergo phase conversion during drying, leaving them vulnerable to rupturing and tearing during sudden volume changes in rehydration [32, 100]. The blastospore cell membrane is no exception to this but can evidently be protected by intracellular trehalose (and glycerol in hyp.+tre. treat.). The significantly smaller PI-ctcf response and the lack of a BOX-ctcf response of hyp.+tre. treat. upon rehydration confirm that trehalose's unique ability to preserve membrane fluidity worked as desired in *M. brunneum* blastospores [38–40, 46]. Figures 2 and 3 suggest that small increases in cellular trehalose and glycerol content, as a result of hyp.+tre. treat., can exponentially lower the experienced stress and death during rehydration.

Figure 3b revealed that blastospores during germ tube formation were especially vulnerable to desiccative stress. More precisely, the germ tube membranes appeared to be the point of failure during desiccation. While in hypotonic + trehalose-treated, protected blastospores this was limited to membrane depolarisation visible through the influx of BOX but not PI, membrane ruptures and the influx of PI were visible in the control. A conceivable reason could be that during germ tube formation and septation, none or only few of the protective solutes were transferred to the newly formed structure [101, 102]. However, no septation is visible in the images, and the localised membrane depolarisation is already visible at the very beginning of germ tube formation (Fig. 3b, red oval). More likely, as phospholipids are inserted into the cell membrane during germ tube growth [103] and at the same time enzymatic and mechanical degradations take place at the cell wall [104], vulnerabilities are created that lead to possibly fatal membrane depolarisation, even before rehydration. This highlights the importance of adequately equipping cells to deal with dehydration, but also reveals the importance of preventing germination before drying if survival is to be maximised.

A real drying process can never be fully emulated by osmotic desiccation. Therefore, to confirm that satisfying all described conditions truly increased desiccation tolerance, the actual drying survival of untreated, trehalose-treated, and hypotonic + trehalose-treated blastospores was measured by CFU analysis. According to Fig. 4, trehalose incubation, either as part of trehalose treatment or hypotonic + trehalose treatment, significantly increased drying survival as expected. Blastospores took in trehalose during incubation and were better set up to survive desiccation. Drying the samples in the residual trehalose solution delivered the highest viability overall. The achieved survival of 51.5% and 71.5%

with trehalose-treated and hypotonic + trehalose-treated blastospores, respectively, seem like acceptable result, but the residual moisture content of the samples (Table 3) must be considered. Samples with residual trehalose did not reach the targeted water activity within the designated timeframe of 48 h. The further a cell is dried, the stronger the adverse effects of water loss become [14]. As a result, the samples with residual trehalose were exposed to less harsh conditions, artificially improving their drying survival, making a direct comparison to samples below the target water activity impossible. In industrial settings, drying to a water activity of less than 0.35 or even less than 0.3 is desired [105]. This, however, clearly demonstrates the challenges of treatments and formulations with trehalose or other strongly hygroscopic substances. Trehalose impedes drying to the water activities necessary for storage, is prone to water reabsorption when dry [106], is sticky in intermediate moisture states [107], and, in this case, had to be removed from the extracellular environment. In addition, any excess sugar in a formulation generally promotes unwanted microbial growth if moisture levels increase. During storage, for example, this would be detrimental to product quality. Therefore, the removal of extracellular trehalose is generally advisable.

In both cases, whether residual trehalose was removed or not, hypotonic + trehalose-treated blastospores displayed significantly higher viability than those of only trehalose-treated blastospores, reaching 40.5% and 71.5% respectively (Fig. 4). This confirms the initial hypothesis that incubation in a hypotonic solution, preceding an incubation in a trehalose solution, would lead to higher viabilities, than just an incubation in a trehalose solution. Furthermore, the previously discussed results paint a detailed picture of intracellular mechanisms during and after hypotonic treatment, ultimately leading to this improved drying stability. The reason likely being the increased trehalose uptake and glycerol synthesis, caused by the lactate release and stress during hypotonic pretreatment.

With recent application-orientated works on desiccation-tolerant blastospore products reporting viabilities of 60% to 80% [25, 26, 105, 108, 109], our achieved viability of 40.5%, when properly dried, falls short in comparison. Several factors, however, must be considered. Selection of strains with high out-of-the-gate desiccation tolerances, strain-optimised fermentation conditions, gentle drying, and optimal, but possibly unrealistic, rehydration conditions all contributed to successfully producing desiccation-tolerant blastospores in those examples [14]. In contrast, the methods at hand were chosen to ensure the observability of the hypotonic + trehalose treatment's effect on desiccation tolerance in isolation, which is necessary to properly evaluate the presented technique. Therefore, only simple, harsh de- and rehydration methods were employed without any constituents. In a more meaningful comparison

with similarly harsh methods, Dietsch et al. [110] achieved a viability of 33% by coating blastospores with polymer layers and Lorenz et al. [111] investigated the isolated effect of formulation additives on alginate bead formulations of *M. brunneum* and achieved a viability of 14.7% with conventional polymer encapsulation. We therefore postulate that there is potential in hypotonic pretreatment to increase desiccation tolerance and that viabilities can be significantly improved with optimisations and a ‘best of’ approach regarding the accompanying methods.

Conclusion and outlook

It could be demonstrated that even relatively small differences in intracellular trehalose concentration and solute composition drastically affect desiccation tolerance and drying survival of *M. brunneum* CB15III blastospores. Small increases in concentration have been shown to yield multiplicatively large improvements. Therefore, increasing the amount of intracellular trehalose and modifying the internal solute composition should always be critical goals in desiccation tolerance engineering. The presented method significantly increased the intracellular trehalose concentration, and that of glycerol, another key fungal solute, without losing significant amounts of mannitol, maltose, or glucose. Furthermore, the apparent metabolism of trehalose during the trehalose incubation of the hypotonic + trehalose treatment indicated that the blastospores synthesised other solutes, like glycerol, to combat the increased osmolarity of the trehalose incubation. Understanding and offering the optimum composition of solutes after hypotonic incubation will allow for a more efficient treatment and likely further increased viabilities post drying and rehydration. It must be noted, however, that such an alteration of the internal conditions could affect virulence, which should be ensured before the application of hyp. + tre.-treated organisms as biocontrol agents.

The fluorescence-based observation of a desiccation and rehydration in a microfluidic environment confirmed the rehydration to be the most damaging phase of a de- and rehydration cycle, upon which hypotonic + trehalose treatment prevented membrane stress and minimised cell death. However, during the prior desiccation, hypotonic + trehalose treatment increased membrane stress and cell death during compared to trehalose treatment, likely because of the stressful switch from a hypo- to hypertonic environment during hypotonic + trehalose treatment. Furthermore, the increased and possibly fatal vulnerability of germ tubes was reported for the first time, and prevention of germ tube formation was identified as a critical goal before drying, next to protective solute accumulation.

Supplementary Information

The online version contains supplementary material available at <https://doi.org/10.1186/s44314-024-00016-z>.

Supplementary Material 1: Fig. 1. First experimental repeat of Fig. 1. The conductivity increase that occurred due to blastospore solute release after media dilution from 154 mM NaCl to 12.32 mM NaCl (hypotonic shock) and after blastospore death and integrity disruption by heat and mechanical stress (death/destruction). The blastospore concentrations are shown on the x axis. No blastospores were present in the control. The data was normalised to the control and the survival rates after hypotonic shock were accounted for in the calculations. $n=5$. According to linear regression, blastospore concentration had a significant influence on delta conductivity for hypotonic shock (adj. $R^2=0.9321$, $F_{1,18}=261.7$, $p=3.623^{-12}$) and death/destruction (adj. $R^2=0.9394$, $F_{1,18}=295.5$, $p=1.292^{-12}$). The effect of concentration was modified by death/destruction of the cells ($p=0.00619$). Fig. 2. Second experimental repeat of Fig. 1. The conductivity increase that occurred due to blastospore solute release after media dilution from 154 mM NaCl to 12.32 mM NaCl (hypotonic shock) and after blastospore death and integrity disruption by heat and mechanical stress (death/destruction). The blastospore concentrations are shown on the x axis. No blastospores were present in the control. The data was normalised to the control and the survival rates after hypotonic shock were accounted for in the calculations. $n=5$. According to linear regression, blastospore concentration had a significant influence on delta conductivity for hypotonic shock (adj. $R^2=0.9571$, $F_{1,18}=424.8$, $p=5.732^{-14}$) and death/destruction (adj. $R^2=0.9322$, $F_{1,18}=262.3$, $p=3.544^{-12}$). The effect of concentration was modified by death/destruction of the cells ($p=0.00585$).

Supplementary Material 2: Fig. 3. Depiction of fold changes analogous to Fig. 2, with an extended range of solutes. Lowercase letters indicate significant differences between the treatments, but not solutes ($n=4$, $p<0.05$). Exact p -values, F -values, χ^2 -values, and employed tests for every solute are given in the Supplementary Materials Table 1. Table 1. Statistical analyses used for GC–MS.

Supplementary Material 3: Fig. 4. More depictions of untreated (A–C) and hypotonic + trehalose-treated (D–F) blastospores at the end of the desiccation ($t=4.5$ h) with visible germ tube growth. The images are compositions of the phase contrast, green, and red fluorescence channel images.

Supplementary Material 4: Table 2. The table shows the estimate increases of the logit model (est.), the standard errors (se) and p -values (p) of all treatments of Fig. 4 towards one another. Stars indicate significance below $p=0,05$. 1 = Trehalose treatment, 2 = hypotonic + trehalose treatment. A = dried in 0.9% NaCl, B = dried in 10% Trehalose. Fig. 5. First experimental repeat of Fig. 4. Lowercase letters indicate statistically significant differences according to a generalised linear model ($n=5$, $p<0.05$). Estimated differences of the logit model, standard errors and exact p -values against all treatments are given in Supplementary Materials Table 3. The data was normalised to the viability of the respective treatment before drying. iqr = interquartile range. Table 3. Statistical analysis of Supplementary Materials Fig. 5. The table shows the estimate increases of the logit model (est.), the standard errors (se) and p -values (p) of all treatments of towards one another. Stars indicate significance below $p=0,05$. Fig. 6. Second experimental repeat of Fig. 4. Lowercase letters indicate statistically significant differences according to a generalised linear model ($n=6$, $p<0.05$). Estimated differences of the logit model, standard errors and exact p -values against all treatments are given in Supplementary Materials Table 3. The data was normalised to the viability of the respective treatment before drying. iqr = interquartile range. Table 4: Statistical analysis of Supplementary Materials Fig. 6. The table shows the estimate increases of the logit model (est.), the standard errors (se) and p -values (p) of all treatments of towards one another. Stars indicate significance below $p=0,05$.

Acknowledgements

This work was funded by the German Federal Ministry of Education and Research (BMBF) as part of the FORK project (FKZ: 13FH118PA8), by Deutsche Forschungsgemeinschaft (DFG, German Research Foundation) – 490988677 – and Hochschule Bielefeld—University of Applied Sciences and Arts.

Authors' contributions

RD devised the topic and all experiments. RD prepared all figures. RD performed the conductivity analysis and drying survival analysis. LBI and RD performed the microfluidic desiccation. MP and RD performed GC–MS. RD wrote the main manuscripts. RD and DSJ interpreted the results of all experiments. DSJ, AG, and AP took on an advisory role throughout the writing of the manuscript. All authors reviewed the manuscript.

Funding

Open Access funding enabled and organized by Projekt DEAL.

Data availability

The raw and processed datasets required to reproduce these findings are available to download from "<https://data.mendeley.com/datasets/x92rbd64cd/1>".

Declarations**Ethics approval and consent to participate**

Not applicable.

Competing interests

The authors declare no competing interests.

Author details

¹WG Fermentation and Formulation of Biologicals and Chemicals, Faculty of Engineering and Mathematics, Hochschule Bielefeld, Bielefeld, Germany. ²Bioengineering and Sustainability, Westfälische Hochschule, Recklinghausen, Germany. ³Multiscale Bioengineering, Technical Faculty, Bielefeld University, Bielefeld, Germany. ⁴OMICS Core Facility – Proteomics Metabolomics Unit (under construction), Bielefeld University, Bielefeld, Germany. ⁵Microbial Genomics and Biotechnology, Center for Biotechnology, Bielefeld University, Bielefeld, Germany. ⁶Institute of Process Engineering in Life Sciences: Microsystems in Bioprocess Engineering, Karlsruhe Institute of Technology, Karlsruhe, Germany.

Received: 28 October 2024 Accepted: 28 December 2024

Published online: 31 January 2025

References

- Mirzabaev A, Kerr RB, Hasegawa T, Pradhan P, Wreford A, von der Pahlen MCT, et al. Severe climate change risks to food security and nutrition. *Clim Risk Manage.* 2023;39:100473.
- Bebber DP, Ramotowski MAT, Gurr SJ. Crop pests and pathogens move polewards in a warming world. *Nat Clim Change.* 2013;3(11):985–8.
- Bebber DP. Range-expanding pests and pathogens in a warming world. *Annu Rev Phytopathol.* 2015;53:335–56.
- Deutsch CA, Tewksbury JJ, Tigchelaar M, Battisti DS, Merrill SC, Huey RB, et al. Increase in crop losses to insect pests in a warming climate. *Science.* 2018;361(6405):916–9.
- Eckert E, Kovalevska O. Sustainability in the European Union: analyzing the discourse of the European green deal. *J Risk Financial Manag.* 2021;14(2):80.
- Tataridas A, Kanas P, Chatzigeorgiou A, Zannopoulos S, Travlos I. Sustainable crop and weed management in the era of the EU Green Deal: a survival guide. *Agronomy.* 2022;12(3):589.
- Fravel DR. Commercialization and implementation of biocontrol. *Annu Rev Phytopathol.* 2005;43:337–59.
- Malusá E, Sas-Paszt L, Ciesielska J. Technologies for beneficial microorganisms inocula used as biofertilizers. *Sci World J.* 2012;2012:491206.
- Parnell JJ, Berka R, Young HA, Sturino JM, Kang Y, Barnhart DM, et al. From the lab to the farm: an industrial perspective of plant beneficial microorganisms. *Front Plant Sci.* 2016;7:1110.
- Sahu PK, Gupta A, Singh M, Mehrotra P, Brahma Prakash GP. Bioformulation and fluid bed drying: a new approach towards an improved biofertilizer formulation. *SpringerLink.* 2018. p. 47–62.
- Krell V, Unger S, Jakobs-Schoenwandt D, Patel AV. Endophytic *Metarhizium brunneum* mitigates nutrient deficits in potato and improves plant productivity and vitality. *Fungal Ecol.* 2018;34:43–9.
- Krell V, Unger S, Jakobs-Schoenwandt D, Patel AV. Importance of phosphorus supply through endophytic *Metarhizium brunneum* for root:shoot allocation and root architecture in potato plants. *Plant Soil.* 2018;430(1–2):87–97.
- Leland JE, Mullins DE, Vaughan LJ, Warren HL. Effects of media composition on submerged culture spores of the entomopathogenic fungus, *Metarhizium anisopliae* var. *acidum* Part 2: Effects of media osmolality on cell wall characteristics, carbohydrate concentrations, drying stability, and pathogenicity. *Biocontrol Sci Technol.* 2005;15(4):393–409.
- Dietsch R, Jakobs-Schönwandt D, Grünberger A, Patel A. Desiccation-tolerant fungal blastospores: from production to application. *Curr Res Biotechnol.* 2021;3:323–39.
- Butt TM, Coates CJ, Dubovskiy IM, Ratcliffe NA. Chapter nine - entomopathogenic fungi: new insights into host–pathogen interactions. *Adv Genet.* 2016;94:307–64.
- Iwanicki NSA, Júnior ID, Eilenberg J, De Fine Licht HH. Comparative RNAseq analysis of the insect-pathogenic fungus *Metarhizium anisopliae* reveals specific transcriptome signatures of filamentous and yeast-like development. *G3.* 2020;10(7):2141–57.
- Valero-Jiménez CA, Wieggers H, Zwaan BJ, Koenraad CJM, van Kan JAL. Genes involved in virulence of the entomopathogenic fungus *Beauveria bassiana*. *J Invertebr Pathol.* 2016;133:41–9.
- Fang W, St. Leger RJ. Mrt, a gene unique to fungi, encodes an oligosaccharide transporter and facilitates rhizosphere competency in *Metarhizium robertsii*. *Plant Physiol.* 2010;154(3):1549–57.
- Xu L, Li J, Gonzalez Ramos VM, Lyra C, Wiebenga A, Grigoriev IV, et al. Genome-wide prediction and transcriptome analysis of sugar transporters in four ascomycete fungi. *Bioresour Technol.* 2024;391:130006.
- Nogueira KMV, de Paula RG, Antoniêto ACC, dos Reis TF, Carraro CB, Silva AC, et al. Characterization of a novel sugar transporter involved in sugarcane bagasse degradation in *Trichoderma reesei*. *Biotechnol Biofuels.* 2018;11(1):84–17.
- Plourde-Owobi L, Durner S, Parrou JL, Wieczorke R, Goma G, François J. AGT1, encoding an α -glucoside transporter involved in uptake and intracellular accumulation of trehalose in *Saccharomyces cerevisiae*. *J Bacteriol.* 1999;181(12):3830–2.
- Kotyka A, Michaljaníková D. Uptake of trehalose by *Saccharomyces cerevisiae*. *Microbiology.* 1979;110(2):323–32.
- Kellogg D. Desiccation tolerance: an unusual window into stress biology. *Mol Biol Cell.* 2019;30(6):737–41.
- Alkhaibari AM, Carolino AT, Yavasoglu SI, Maffei T, Mattoso TC, Bull JC, et al. *Metarhizium brunneum* Blastospore pathogenesis in *Aedes aegypti* larvae: attack on several fronts accelerates mortality. *PLoS Pathog.* 2016;12:e1005715.
- Mascarin GM, Jackson MA, Behle RW, Kobori NN, Delalibera I. Improved shelf life of dried *Beauveria bassiana* blastospores using convective drying and active packaging processes. *Appl Microbiol Biot.* 2016;100(19):8359–70.
- Iwanicki NSA, Ferreira BDO, Mascarin GM, Delalibera Junior I. Modified Adamek's medium renders high yields of *Metarhizium robertsii* blastospores that are desiccation tolerant and infective to cattle-tick larvae. *Fungal Biol.* 2018;122(9):883–90.
- Iwanicki NSA, Mascarin GM, Moreno SG, Eilenberg J, Júnior ID. Growth kinetic and nitrogen source optimization for liquid culture fermentation of *Metarhizium robertsii* blastospores and bioefficacy against the corn leafhopper *Dalbulus maidis*. *World J Microbiol Biotechnol.* 2020;36(5):1–13.
- Corrêa B, da Silveira DV, Silva DM, Mascarin GM, Júnior ID. Comparative analysis of blastospore production and virulence of *Beauveria bassiana* and *Cordyceps fumosorosea* against soybean pests. *Biocontrol.* 2020;65(3):323–37.
- Morales-Reyes C, Mascarin GM, Jackson MA, Hall D, Sánchez-Peña SR, Arthurs SP. Comparison of aerial conidia and blastospores from two entomopathogenic fungi against *Diaphorina citri* (Hemiptera: Liviidae) under laboratory and greenhouse conditions. *Biocontrol Sci Technol.* 2018;28(8):737–49.
- Jaronski S. Mass production of entomopathogenic fungi—state of the art. In: Morales-Ramos JA, Guadalupe Rojas M, Shapiro-Ilan DI, editors. *Mass production of beneficial organisms: invertebrates and entomopathogens.* 1st ed. San Diego: Academic Press; 2013. p. 357–413.

31. Mascarin GM, Jackson MA, Kobori NN, Behle RW, Delalibera Jf. Liquid culture fermentation for rapid production of desiccation tolerant blastospores of *Beauveria bassiana* and *Isaria fumosorosea* strains. *J Invertebr Pathol.* 2015;127:11–20.
32. Lebre PH, De Maayer P, Cowan DA. Xerotolerant bacteria: surviving through a dry spell. *Nat Rev Microbiol.* 2017;15(5):285–96.
33. Pade N, Hagemann M. Salt acclimation of cyanobacteria and their application in biotechnology. *Life.* 2015;5(1):25.
34. Esbelin J, Santos T, Hébraud M. Desiccation: an environmental and food industry stress that bacteria commonly face. *Food Microbiol.* 2018;69:82–8.
35. Potts M, Slaughter SM, Hunneke F-U, Garst JF, Helm RF. Desiccation tolerance of prokaryotes: application of principles to human cells. *Integr Comp Biol.* 2005;45(5):800–9.
36. Jain NK, Roy I. Effect of trehalose on protein structure. *Protein Sci.* 2009;18(1):24.
37. Crowe JH, Oliver AE, Tablin F. Is there a single biochemical adaptation to anhydrobiosis? *Integr Comp Biol.* 2002;42(3):497–503.
38. Crowe JH. Water, membranes, and life without water. In: Le Bihan D, Fukuyama H, editors. *Water: the forgotten biological molecule.* 1st ed. Singapore: Pan Stanford Publishing; 2010. p. 205–29.
39. Sleator RD, Hill C. Bacterial osmoadaptation: the role of osmolytes in bacterial stress and virulence. *FEMS Microbiol Rev.* 2002;26(1):49–71.
40. Leslie SB, Israeli E, Lighthart B, Crowe JH, Crowe LM. Trehalose and sucrose protect both membranes and proteins in intact bacteria during drying. *Appl Environ Microb.* 1995;61(10):3592–7.
41. Chakrabortee S, Boschetti C, Walton LJ, Sarkar S, Rubinsztein DC, Tunnacliffe A. Hydrophilic protein associated with desiccation tolerance exhibits broad protein stabilization function. *Proc Natl Acad Sci U S A.* 2007;104(46):18073–8.
42. Janis B, Belott C, Menze MA. Role of intrinsic disorder in animal desiccation tolerance. *Proteomics.* 2018;18(21–22):1800067.
43. Shimizu T, Kanamori Y, Furuki T, Kikawada T, Okuda T, Takahashi T, et al. Desiccation-induced structuralization and glass formation of group 3 late embryogenesis abundant protein model peptides. *Biochemistry.* 2010;49(6):1093–104.
44. Bokor M, Cszizmok V, Kovacs D, Banki P, Friedrich P, Tompa P, et al. NMR relaxation studies on the hydrate layer of intrinsically unstructured proteins. *Biophys J.* 2005;88:2030–7.
45. Laskowska E, Kuczyńska-Wiśnik D. New insight into the mechanisms protecting bacteria during desiccation. *Curr Genet.* 2020;66(2):313–8.
46. Kumar A, Cincotti A, Aparicio S. Insights into the interaction between lipid bilayers and trehalose aqueous solutions. *J Mol Liq.* 2020;314:113639.
47. Ramirez JF, Kumara UGVSS, Arulsamy N, Boothby TC. Water content, transition temperature and fragility influence protection and anhydrobiotic capacity. *BBA Adv.* 2024;5:100115.
48. Crowe JH, Carpenter JF, Crowe LM. The role of vitrification in anhydrobiosis. *Annu Rev Physiol.* 1998;60(1):73–103.
49. Van Dijck P, Colavizza D, Smet P, Thevelein JM. Differential importance of trehalose in stress resistance in fermenting and nonfermenting *Saccharomyces cerevisiae* cells. *Appl Environ Microb.* 1995;61(1):109–15.
50. Drake AC, Lee Y, Burgess EM, Karlsson JOM, Eroglu A, Higgins AZ. Effect of water content on the glass transition temperature of mixtures of sugars, polymers, and penetrating cryoprotectants in physiological buffer. *PLoS One.* 2018;13(1):e0190713.
51. Li HX, Lee BH. Enhanced conidial thermotolerance and field efficacy of *Beauveria bassiana* by saccharides. *Biotechnol Lett.* 2014;36(12):2481–8.
52. Tapia H, Young L, Fox D, Bertozzi CR, Koshland D. Increasing intracellular trehalose is sufficient to confer desiccation tolerance to *Saccharomyces cerevisiae*. *Proc Natl Acad Sci U S A.* 2015;112(19):6122–7.
53. Potts M. Desiccation tolerance of prokaryotes. *Microbiol Rev.* 1994;58(4):755–805.
54. Cruz Barrera M, Jakobs-Schoenwandt D, Persicke M, Gómez MI, Ruppel S, Patel AV. Anhydrobiotic engineering for the endophyte bacterium *Kosakonia radicincitans* by osmoadaptation and providing exogenously hydroxyectoine. *World J Microbiol Biotechnol.* 2019;36(1):6.
55. Tarocco F, Lecuona RE, Couto AS, Arcas JA. Optimization of erythritol and glycerol accumulation in conidia of *Beauveria bassiana* by solid-state fermentation, using response surface methodology. *Appl Microbiol Biot.* 2005;68(4):481–8.
56. Mascarin GM, Jackson MA, Kobori NN, Behle RW, Dunlap CA, Júnior ID. Glucose concentration alters dissolved oxygen levels in liquid cultures of *Beauveria bassiana* and affects formation and bioefficacy of blastospores. *Appl Microbiol Biot.* 2015;99(16):6653–65.
57. Jaronski ST, Mascarin GM. Mass production of fungal entomopathogens. In: Lacey LA, editor. *Microbial control of insect and mite pests: from theory to practice.* London: Elsevier Science; 2016. p. 141–56.
58. Hohmann S. Osmotic stress signaling and osmoadaptation in yeasts. *Microbiol Mol Biol Rev.* 2002;66(2):300.
59. Tamás MJ, Luyten K, Sutherland FCW, Hernandez A, Albertyn J, Valadi H, et al. Fps1p controls the accumulation and release of the compatible solute glycerol in yeast osmoregulation. *Mol Microbiol.* 1999;31(4):1087–104.
60. Booth IR, Louis P. Managing hypoosmotic stress: aquaporins and median-sensitive channels in *Escherichia coli*. *Curr Opin Microbiol.* 1999;2(2):166–9.
61. Bahnemann J, Grünberger A. Microfluidics in biotechnology: overview and status quo. *Adv Biochem Eng Biotechnol.* 2022;179:1–16.():Adv.
62. Krell V, Jakobs-Schoenwandt D, Vidal S, Patel AV. Encapsulation of *Metarhizium brunneum* enhances endophytism in tomato plants. *Biol Control.* 2018;116:62–73.
63. Kováts E. Gas-chromatographische Charakterisierung organischer Verbindungen. Teil 1: Retentionsindices aliphatischer Halogenide, Alkohole, Aldehyde und Ketone. *Helv Chim Acta.* 1958;41(7):1915–32.
64. Plassmeier J, Barsch A, Persicke M, Niehaus K, Kalinowski J. Investigation of central carbon metabolism and the 2-methylcitrate cycle in *Corynebacterium glutamicum* by metabolic profiling using gas chromatography–mass spectrometry. *J Biotechnol.* 2007;130(4):354–63.
65. Hummel J, Strehmel N, Selbig J, Walther D, Kopka J. Decision tree supported substructure prediction of metabolites from GC-MS profiles. *Metabolomics.* 2010;6(2):322–33.
66. Kopka J, Schauer N, Krueger S, Birkemeyer C, Usadel B, Bergmüller E, et al. GMD@CSB.DB: the Golm metabolome database. *Bioinformatics.* 2005;21(8):1635–8.
67. Schauer N, Steinhäuser D, Strelkov S, Schomburg D, Allison G, Moritz T, et al. GC-MS libraries for the rapid identification of metabolites in complex biological samples. *FEBS Lett.* 2005;579(6):1332–7.
68. Blöbaum L, Täuber S, Grünberger A. Protocol to perform dynamic microfluidic single-cell cultivation of *C. glutamicum*. *STAR Protoc.* 2023;4(3):102436.
69. Täuber S, Blöbaum L, Steier V, Oldiges M, Grünberger A. Microfluidic single-cell scale-down bioreactors: a proof-of-concept for the growth of *Corynebacterium glutamicum* at oscillating pH values. *Biotechnol Bioeng.* 2022;119(11):3194–209.
70. Simonin H, Beney L, Gervais P. Sequence of occurring damages in yeast plasma membrane during dehydration and rehydration: mechanisms of cell death. *Biochim Biophys Acta.* 2007;1768(6):1600–10.
71. Krämer CEM, Wiechert W, Kohlheyer D. Time-resolved, single-cell analysis of induced and programmed cell death via non-invasive propidium iodide and counterstain perfusion. *Sci Rep.* 2016;6:32104.
72. Schindelin J, Arganda-Carreras I, Frise E, Kaynig V, Longair M, Pietzsch T, et al. Fiji: an open-source platform for biological-image analysis. *Nat Methods.* 2012;9(7):676–82.
73. El-Sharkawey AE. Calculate the corrected total cell fluorescence (CTCF). ResearchGate. 2016.
74. R Core Team. R: a language and environment for statistical computing. Vienna, Austria: R Foundation for Statistical Computing; 2021.
75. Ritz C, Baty F, Streibig JC, Gerhard D. Dose-response analysis using R. *Plos One.* 2015;10(12):e0146021.
76. Kassambara A. rstatix: pipe-friendly framework for basic statistical tests. R package. 0.7.2. ed. 2023.
77. Fox JWS. An R companion to applied regression. 3rd ed. Thousand Oaks: Sage; 2019.
78. Hothorn T, Bretz F, Westfall P. Simultaneous inference in general parametric models. *Biom J.* 2008;50(3):346–63.
79. Asami K, Hanai T, Koizumi N. Dielectric properties of yeast cells. *J Membr Biol.* 1976;28(1):169–80.
80. Mucchetti G, Gatti M, Neviani E. Electrical conductivity changes in milk caused by acidification: determining factors. *J Dairy Sci.* 1994;77(4):940–4.
81. Meaney PM, Fox CJ, Geimer SD, Paulsen KD. Electrical characterization of glycerin: water mixtures: implications for use as a coupling medium in microwave tomography. *IEEE Trans Microwave Theory Tech.* 2017;65(5):1471.

82. Chen HH, Zhou X, Shu Z, Woods EJ, Gao D. Electrical conductivity measurements for the ternary systems of glycerol/sodium chloride/water and ethylene glycol/sodium chloride/water and their applications in cryopreservation. *Biopreserv Biobank*. 2009;7(1):13–8.
83. Payot T, Fick M. On-line estimation of lactic acid concentration by conductivity measurement in fermentation broth. *Biotechnol Tech*. 1997;11(1):17–20.
84. Liaud N, Giniés C, Navarro D, Fabre N, Crapart S, Gimbert IH, et al. Exploring fungal biodiversity: organic acid production by 66 strains of filamentous fungi. *Fungal Biol Biotechnol*. 2014;1(1):1–10.
85. Pascual S, Melgarejo P, Magan N. Accumulation of compatible solutes in penicillium frequentans grown at reduced water activity and biocontrol of *Monilinia laxa*. *Biocontrol Sci Technol*. 2000;10(1):71–80.
86. Teixidó, Vinas, Usall, Sanchis, Magan. Ecophysiological responses of the biocontrol yeast *Candida sake* to water, temperature and pH stress. *J Appl Microbiol*. 1998;84(2):192–200.
87. Beales N. Adaptation of microorganisms to cold temperatures, weak acid preservatives, low pH, and osmotic stress: a review. *Compr Rev Food Sci F*. 2004;3(1):1–20.
88. Hallsworth JE, Magan N. Manipulation of intracellular glycerol and erythritol enhances germination of conidia at low water availability. *Microbiology*. 1995;141(5):1109–15.
89. Krell V, Jakobs-Schoenwandt D, Persicke M, Patel AV. Endogenous arabitol and mannitol improve shelf life of encapsulated *Metarhizium brunneum*. *World J Microbiol Biotechnol*. 2018;34(8):108.
90. Clegg JS, Seitz P, Seitz W, Hazlewood CF. Cellular responses to extreme water loss: the water-replacement hypothesis. *Cryobiology*. 1982;19(3):306–16.
91. Grasmeyer N, Stankovic M, de Waard H, Frijlink HW, Hinrichs WLJ. Unraveling protein stabilization mechanisms: vitrification and water replacement in a glass transition temperature controlled system. *Biochim Biophys Acta*. 2013;1834(4):763–9.
92. Golovina EA, Golovin AV, Hoekstra FA, Faller R. Water replacement hypothesis in atomic detail—factors determining the structure of dehydrated bilayer stacks. *Biophys J*. 2009;97(2):490.
93. Hallsworth J, Magan N. Improved biological control by changing polyols/ trehalose in conidia of entomopathogens. Brighton crop protection conference-pests and diseases. Brighton, England. Belfast (IE); 1994. p. 1091–6.
94. Weng L, Elliott GD. Local minimum in fragility for trehalose/glycerol mixtures: implications for biopharmaceutical stabilization. *J Phys Chem B*. 2015;119(22):6820–7.
95. Attfield PV. Stress tolerance: the key to effective strains of industrial baker's yeast. *Nat Biotechnol*. 1997;15(13):1351–7.
96. Lillie SH, Pringle JR. Reserve carbohydrate metabolism in *Saccharomyces cerevisiae*: responses to nutrient limitation. *J Bacteriol*. 1980;143(3):1384–94.
97. Hallsworth JE, Magan N. Culture age, temperature, and pH affect the polyol and trehalose contents of fungal propagules. *Appl Environ Microb*. 1996;62(7):2435–42.
98. Hallsworth JE, Magan N. Effect of carbohydrate type and concentration on polyhydroxy alcohol and trehalose content of conidia of three entomopathogenic fungi. *Microbiology*. 1994;140(10):2705–13.
99. Hallsworth JE, Magan N. Effects of KCl concentration on accumulation of acyclic sugar alcohols and trehalose in conidia of three entomopathogenic fungi. *Lett Appl Microbiol*. 1994;18(1):8–11.
100. Crowe JH, Hoekstra FA, Crowe LM. Anhydrobiosis. *Annu Rev Physiol*. 1992;54(1):579–99.
101. Uribe DU, Khachatourians GGKG. Identification and characterization of an alternative oxidase in the entomopathogenic fungus *Metarhizium anisopliae*. *Can J Microbiol*. 2008;54(2):119–27.
102. Mongkolsamrit S, Khonsanit A, Thanakitpipattana D, Tasanathai K, Noisripoom W, Lamlerthton S, et al. Revisiting *Metarhizium* and the description of new species from Thailand. *Stud Mycol*. 2020;95:171–251.
103. Vermaas JV, Tajkhorshid E. A microscopic view of phospholipid insertion into biological membranes. *J Phys Chem B*. 2014;118(7):1754.
104. Cassone A, Simonetti N, Strippoli V. Ultrastructural changes in the wall during germ-tube formation from blastospores of *Candida albicans*. *Microbiology*. 1973;77(2):417–26.
105. Jackson MA, Mascarin GM, inventors; EMBRAPA, US Department of Agriculture assignee. Stable fungal blastospores and methods for their production, stabilization and use. Canada; 2016.
106. Mah PT, O'Connell P, Focaroli S, Lundy R, O'Mahony TF, Hastedt JE, et al. The use of hydrophobic amino acids in protecting spray dried trehalose formulations against moisture-induced changes. *Eur J Pharm Biopharm*. 2019;144:139–53.
107. Kopjar M, Pilizota V, Hribar J, Tiban NN, Subaric D, Babic J, et al. Influence of trehalose addition on instrumental textural properties of strawberry pastes. *Int J Food Prop*. 2008;11(3):646–55.
108. Iwanicki NSA, Mascarin GM, Moreno SG, Ellenberg J, Delalibera I. Development of novel spray-dried and air-dried formulations of *Metarhizium robertsii* blastospores and their virulence against *Dalbulus maidis*. *Appl Microbiol Biotechnol*. 2021;105(20):7913–33.
109. Mascarin GM, Kobori NN, Jackson MA, Dunlap CA, Delalibera I. Nitrogen sources affect productivity, desiccation tolerance and storage stability of *Beauveria bassiana* blastospores. *J Appl Microbiol*. 2018;124(3):810–20.
110. Dietsch R, Jakobs-Schönwandt D, Blöbaum L, Bondzio L, Grünberger A, Patel A. Single-cell polymer coating improves the desiccation tolerance of *Metarhizium brunneum* blastospores. *Biotechnol Environ*. 2024;1(1):1–15.
111. Lorenz S-C, Humbert P, Patel AV. Chitin increases drying survival of encapsulated *Metarhizium pemphigi* blastospores for Ixodes ricinus control. *Ticks Tick-borne Dis*. 2020;11(6):101537.

Publisher's Note

Springer Nature remains neutral with regard to jurisdictional claims in published maps and institutional affiliations.